

A Comparative Analysis of Isotropic and Anisotropic Features on Natural Convection in a Permeable Cavity

Pallath Chandran¹, Nirmal C. Sacheti¹, Ashok K. Singh², B. S. Bhadauria³

¹Department of Mathematics, College of Science, Sultan Qaboos University, PC 123, Al Khod, Muscat, Sultanate of Oman.

²Department of Mathematics, Institute of Science, Banaras Hindu University, Varanasi 221005, India.

³Department of Mathematics, School of Physical Sciences, Babasaheb Bhimrao Ambedkar University, Lucknow 226025, (U.P.), India.

ORCID: 0000-0003-0105-0870 (Pallath Chandran), 0000-0003-0124-0586 (Nirmal C. Sacheti)

Abstract:

The natural convection process occurring in finite cavities is a subject of great research interest in many technological applications. When the cavity has 4-sided walls, the thermal conditions prevailing on these boundaries play significant roles on the flow and thermal characteristics. There are a number of applications where the thermal wall conditions are typically adiabatic on the side vertical walls while the lower and upper walls are isothermal with different temperatures. Moreover, depending upon the nature of applications, one has to consider the isotropic or anisotropic features of the hydrodynamical and thermal characteristics of the porous material. This paper deals with steady laminar natural convective Darcian flow of a viscous incompressible fluid in a finite trapezoidal cavity whose side walls are vertical and the upper wall is slanted. The vertical side walls of the cavity are assumed to be subject to no heat flux condition while the remaining walls are kept at uniform temperatures. We have solved numerically the governing non-dimensional partial differential equations together with the appropriate sets of boundary conditions for velocity and temperature. In order to bring out the salient features of non-isotropy versus isotropy, the effects of a number of important non-dimensional quantities, namely, Rayleigh-Darcy number, aspect ratio, inclination parameter, permeability ratio and thermal diffusivity ratio parameters have been discussed in relation to the streamlines and isotherms.

AMS subject classification: 76S05, 76R10, 80A20.

Keywords: Porous media, natural convection, isotropy, anisotropy, Darcy law, streamlines, isotherms

1. INTRODUCTION

Natural convective flows of viscous fluids in finite enclosures are encountered in several engineering and industrial applications such as heating and cooling of buildings, electronic devices used for cooling purposes, production of geothermal energy from reservoirs, and filtration, among others. In applications involving porous media flows, it is common practice in literature to consider and distinguish between isotropic and anisotropic features of the underlying porous bed with a view to bring out the added influence of anisotropy vis-à-vis isotropy in its physical and thermal

descriptions. It is known that the permeability and thermal diffusivity of a permeable medium can be considered to be isotropic or anisotropic depending on the geometrical, physical and thermal conditions relevant to an application. The importance of the orientations of the principal axes with regard to permeability and thermal diffusivity thus cannot be overlooked. In view of the inherent difficulties of theoretically analyzing porous media flows, it is common practice in the literature to assume the porous bed to be isotropic. However, there are a number of applications wherein the anisotropic nature of the permeability and thermal diffusivity of the porous matrix becomes important. Anisotropy of the permeability in a porous medium is a consequence of the orientation and shape of the pores constituting the porous bed. This in turn renders the heat transfer features also direction dependent.

In the literature, a large number of mathematical models have been employed and analyzed to investigate the influence of anisotropic properties of porous media in natural convective flows [1–5]. In such investigations, one has to take into consideration the orientation of the principal axes. However, the orientation of the principal axes varies from one application to another. For instance, in several studies, one of the principal axes of the anisotropic porous matrix has been assumed to be oriented in the vertical direction while in some other applications, this orientation could even be variable [6, 7].

Another important factor one has to consider in the flow and heat transfer of natural convection studies of viscous fluids in vertical enclosures, is concerned with the applied thermal conditions on the bounding walls in addition to the anisotropic features of the porous bed, see, e.g., [8–19]. These thermal conditions depend very much on the specific type of engineering or industrial problem being investigated. Some of the well-known thermal conditions on the boundaries of the enclosures considered in the literature correspond to the walls being adiabatic or isothermal. The walls of the enclosure could also be subject to ramped temperature, Newtonian heating, Robin condition, etc. It is also pertinent to analyze the effect of a specific thermal condition on a particular bounding wall since the influence of buoyancy forces arising out of the heating or cooling or heat flux at different walls usually lead to different flow and heat transfer features in the cavity. Keeping these in view, we have investigated the coupled effects of thermal forces and anisotropy of the porous bed on the flow and heat transfer of a viscous incompressible fluid inside a trapezoidal

porous cavity in which the upper bounding wall is sloping at an angle θ to the horizontal. The present study is a sequel to the work reported in [18, 19]. Our main focus in this study is to directly compare some salient features of the isotropic versus anisotropic features of the permeable medium on the flow and heat transfer characteristics.

A brief physical description of the problem and its mathematical formulations for the isotropic and anisotropic cases are given in Sections 2–4. In Section 5, the numerical solution procedure of the governing equations has been presented. In the last Section 6, we have exhibited the streamlines and isotherms of the convective flow for some representative values of the governing parameters. The influence of anisotropy in the porous medium has been discussed in comparison to the corresponding isotropic case.

2. PHYSICAL DESCRIPTION

It is well-known that the flow and heat transfer features of a fluid passing through a porous medium are complex, and are considerably modified from the conventional flows. The complexity of the flows arise due primarily to the nonlinear nature of the governing partial differential equations and the associated boundary conditions. When the underlying medium is subject to anisotropic features, the analysis of the ensuing flow becomes much more complicated. However, as indicated in the previous section, flows through anisotropic media are widely encountered in a number of practical applications. In the following, we have thus analyzed the steady free convective flow in a non-rectangular trapezoidal cavity of width L and height H , which is filled with a porous material whose permeability and thermal conductivity are both assumed to be anisotropic. With respect to the 2-D Cartesian coordinate system Oxy , we assume that the y -axis is along the left vertical wall of the cavity while the x -axis is along the horizontal lower side. The sloping upper surface of the cavity is inclined at an angle θ to the horizontal. As regards the thermal conditions on the walls of the enclosure, the vertical surfaces of the enclosure are taken as adiabatic while the lower and upper surfaces are maintained at constant temperatures T_h and T_c , respectively. It is further assumed that $T_h > T_c$, which induces natural convection within the enclosure. As stated above, our main aim in this work is to compare the effects of isotropic versus anisotropic features of the porous medium properties of permeability and thermal diffusivity on the flow and heat transfer. To this end, we shall first present the equations governing the isotropic flow and thereafter the corresponding equations of anisotropic case will be presented. We then compare the differences in flow and heat transfer features induced by anisotropy in an otherwise isotropic flow.

3. GOVERNING EQUATIONS FOR ISOTROPIC CASE

The usual equations of continuity, momentum and energy for the flow in the isotropic porous medium are given by

$$\nabla \cdot \mathbf{V} = 0 \quad (1)$$

$$\mu \mathbf{V} + \kappa (\nabla p + \rho g \vec{j}) = 0 \quad (2)$$

$$(\mathbf{V} \cdot \nabla) T - \lambda (\nabla^2 T) = 0 \quad (3)$$

where \mathbf{V} is the flow velocity, μ the viscosity, κ the permeability of the porous medium, p the pressure, g the gravitational acceleration, λ the thermal diffusivity, and T is the temperature.

In order to transform the governing equations to non-dimensional forms, we write

$$\begin{aligned} (\tilde{x}, \tilde{y}) &= (x/L, y/L), & (\tilde{u}, \tilde{v}) &= (Lu/\lambda, Lv/\lambda) \\ \tilde{T} &= \frac{T - T_c}{T_h - T_c} & R_1 &= \rho_0 g \beta \kappa L (T_h - T_c) / (\mu \lambda) \end{aligned} \quad (4)$$

In the above, R_1 is called the Rayleigh-Darcy number. The quantity β , appearing in the expression for R_1 , is the coefficient of thermal expansion, which arises from the Boussinesq approximation whereby one expresses the variation of fluid density ρ in the form

$$\rho = \rho_0 [1 - \beta(T - T_c)] \quad (5)$$

Obviously, the important parameter quantity R_1 exhibits the combined effects of buoyancy and permeability. We now introduce the stream function Ψ defined by $u = \partial \Psi / \partial y$, $v = -\partial \Psi / \partial x$. It can be verified that the continuity equation (1) is satisfied by Ψ . Using Eq (4) and the stream function, Eqs (1)–(3) can be re-expressed in the following non-dimensional forms (neglecting the “tilde” on the quantities, for convenience):

$$\frac{\partial^2 \Psi}{\partial x^2} + \frac{\partial^2 \Psi}{\partial y^2} = -R_1 \frac{\partial T}{\partial x} \quad (6)$$

$$u \frac{\partial T}{\partial x} + v \frac{\partial T}{\partial y} = \frac{\partial^2 T}{\partial x^2} + \frac{\partial^2 T}{\partial y^2} \quad (7)$$

The boundary conditions relevant to the problem, in non-dimensional form, become

$$\begin{aligned} \Psi &= 0 \text{ on all boundaries} \\ T &= 1 \text{ at } f_3(x, y) = 0 \text{ and } T = 0 \text{ at } f_4(x, y) = 0 \\ \frac{\partial T}{\partial n} &= 0 \text{ at } f_1(x, y) = 0 \text{ and } f_2(x, y) = 0 \end{aligned} \quad (8)$$

where the functions f_1 , f_2 , f_3 and f_4 represent boundaries of the physical trapezoidal domain, and n is the normal to the corresponding boundaries [19].

4. GOVERNING EQUATIONS FOR ANISOTROPIC CASE

When the porous material is anisotropic in both permeability and thermal diffusivity, these quantities are denoted by the tensors K_{xy} and α_{xy} , respectively, and are given by

$$K_{xy} = \begin{bmatrix} K_x & 0 \\ 0 & K_y \end{bmatrix}, \quad \alpha_{xy} = \begin{bmatrix} \alpha_x & 0 \\ 0 & \alpha_y \end{bmatrix} \quad (9)$$

where the quantities with the subscripts have their usual meanings. The counterparts of the governing equations (1)–(3) of the isotropic case, modified for the anisotropic porous medium, now become

$$\nabla \cdot \mathbf{V} = 0 \quad (10)$$

$$\mu \mathbf{V} + K_{xy} (\nabla p + \rho g \vec{j}) = 0 \quad (11)$$

$$(\mathbf{V} \cdot \nabla) T - \nabla \cdot (\alpha_{xy} \nabla T) = 0 \quad (12)$$

where the symbols have the same meaning as in Section 3.

The non-dimensionalization process of Eqs (10)–(12) follows the same procedure as in Eq (4) except that we now have to introduce new non-dimensional quantities to account for the anisotropic features of the porous medium. We thus define two new quantities K and α — ratios of the tensor components of permeabilities and thermal diffusivities, respectively — and re-define the non-dimensional velocity components and the Rayleigh-Darcy number also. These are given by

$$\begin{aligned} K &= K_x/K_y, & \alpha &= \alpha_x/\alpha_y \\ (\tilde{u}, \tilde{v}) &= (Lu/\alpha_y, Lv/\alpha_y), \\ R_2 &= \rho_0 g \beta L K_x (T_h - T_c) / (\mu \alpha_y) \end{aligned} \quad (13)$$

In terms of the stream function Ψ , the counterpart of Eq (6) now becomes

$$K \frac{\partial^2 \Psi}{\partial x^2} + \frac{\partial^2 \Psi}{\partial y^2} = -R_2 \frac{\partial T}{\partial x} \quad (14)$$

while the energy equation assumes the form

$$u \frac{\partial T}{\partial x} + v \frac{\partial T}{\partial y} = \alpha \frac{\partial^2 T}{\partial x^2} + \frac{\partial^2 T}{\partial y^2} \quad (15)$$

The boundary conditions remain the same as Eq (8) in Section 3.

5. SOLUTION PROCEDURE

In this section, we shall describe briefly the main steps in the solution procedure. We shall do this first for the anisotropic case. The boundary value problem described by Eqs (14), (15) and (8) are solved using an algebraic grid generation method combined with a finite difference method. To this end, the trapezoidal physical domain is transformed to a regular unit square domain [18, 19]. This is accomplished by introducing a set of new independent variables ξ and η :

$$\xi = \xi(x, y), \quad \eta = \eta(x, y) \quad (16)$$

where $0 \leq \xi, \eta \leq 1$. Following [18–20], ξ and η can be written as

$$\xi = \frac{x - f_1(x, y)}{f_2(x, y) - f_1(x, y)} \quad (17)$$

$$\eta = \frac{y - f_3(x, y)}{f_4(x, y) - f_3(x, y)} \quad (18)$$

where $f_i(x, y) = 0$, ($i = 1 \dots 4$) represent the boundaries of the physical domain. A detailed description of the

algebraic grid generation method is available in [21]. Using the transformations (17) and (18), one can obtain the relation between the physical and computational domains [18]. We shall first perform the numerical computation in the transformed unit square domain. For this, we transform Eqs (14), (15) and (8) from the physical xy -domain to the computational $\xi\eta$ -domain using the transformation

$$\begin{bmatrix} \frac{\partial \varphi}{\partial x} \\ \frac{\partial \varphi}{\partial y} \end{bmatrix} = \begin{bmatrix} \frac{\partial \xi}{\partial x} & \frac{\partial \eta}{\partial x} \\ \frac{\partial \xi}{\partial y} & \frac{\partial \eta}{\partial y} \end{bmatrix} \begin{bmatrix} \frac{\partial \varphi}{\partial \xi} \\ \frac{\partial \varphi}{\partial \eta} \end{bmatrix} \quad (19)$$

Using Eq (19), Eqs (14) and (15) can be transformed in the forms

$$\begin{aligned} b_1(K) \frac{\partial^2 \Psi}{\partial \xi^2} + b_2(K) \frac{\partial^2 \Psi}{\partial \eta^2} + b_3(K) \frac{\partial^2 \Psi}{\partial \xi \partial \eta} + b_4(K) \frac{\partial \Psi}{\partial \xi} \\ + b_5(K) \frac{\partial \Psi}{\partial \eta} = -R_2 \left(a_1 \frac{\partial T}{\partial \xi} + a_2 \frac{\partial T}{\partial \eta} \right) \end{aligned} \quad (20)$$

$$\begin{aligned} \{a_1 u + a_3 v - b_4(\alpha)\} \frac{\partial T}{\partial \xi} + \{a_2 u + a_4 v - b_5(\alpha)\} \frac{\partial T}{\partial \eta} \\ = b_1(\alpha) \frac{\partial^2 T}{\partial \xi^2} + b_2(\alpha) \frac{\partial^2 T}{\partial \eta^2} + b_3(\alpha) \frac{\partial^2 T}{\partial \xi \partial \eta} \end{aligned} \quad (21)$$

where the functionals $a_1, \dots, a_4, b_1, \dots, b_4$ are defined as

$$\begin{aligned} a_1 &= \frac{\partial \xi}{\partial x}, \quad a_2 = \frac{\partial \eta}{\partial x}, \quad a_3 = \frac{\partial \xi}{\partial y}, \quad a_4 = \frac{\partial \eta}{\partial y}, \\ b_1(s) &= s a_1^2 + a_3^2, \quad b_2(s) = s a_2^2 + a_4^2, \quad b_3(s) = 2(s a_1 a_2 + a_3 a_4), \\ b_4(s) &= 2 \left(s \frac{\partial^2 \xi}{\partial x^2} + \frac{\partial^2 \xi}{\partial y^2} \right), \quad b_5(s) = 2 \left(s \frac{\partial^2 \eta}{\partial x^2} + \frac{\partial^2 \eta}{\partial y^2} \right), \end{aligned} \quad (22)$$

s being either of K or α . The components of velocity, u and v , can be obtained using

$$u = a_3 \frac{\partial \Psi}{\partial \xi} + a_4 \frac{\partial \Psi}{\partial \eta}, \quad v = - \left(a_1 \frac{\partial \Psi}{\partial \xi} + a_2 \frac{\partial \Psi}{\partial \eta} \right) \quad (23)$$

The physical boundary conditions, when transformed into the unit square domain, become

$$\begin{aligned} \Psi &= 0 \quad \text{on all boundaries,} \\ T &= 1 \text{ at } \eta = 0 \text{ and } T = 0 \text{ at } \eta = 1, \\ (a_1 \eta_x + a_3 \eta_y) \frac{\partial T}{\partial \xi} + (a_2 \eta_x + a_4 \eta_y) \frac{\partial T}{\partial \eta} &= 0 \text{ at } \xi = 0 \text{ and } \xi = 1 \end{aligned} \quad (24)$$

For the flow and heat transfer in the isotropic porous medium, a similar procedure as stated above is employed. In this case Eqs (6) and (7), in conjunction with Eq (19), transform, respectively, to

$$\begin{aligned} \beta_1 \frac{\partial^2 \Psi}{\partial \xi^2} + \beta_2 \frac{\partial^2 \Psi}{\partial \eta^2} + \beta_3 \frac{\partial^2 \Psi}{\partial \xi \partial \eta} + \beta_4 \frac{\partial \Psi}{\partial \xi} + \beta_5 \frac{\partial \Psi}{\partial \eta} \\ = -R_1 \left(a_1 \frac{\partial T}{\partial \xi} + a_2 \frac{\partial T}{\partial \eta} \right) \end{aligned} \quad (25)$$

$$\{a_1u + a_3v - \beta_4\} \frac{\partial T}{\partial \xi} + \{a_2u + a_4v - \beta_5\} \frac{\partial T}{\partial \eta} \quad (26)$$

$$= \beta_1 \frac{\partial^2 T}{\partial \xi^2} + \beta_2 \frac{\partial^2 T}{\partial \eta^2} + \beta_3 \frac{\partial^2 T}{\partial \xi \partial \eta}$$

where

$$a_1 = \frac{\partial \xi}{\partial x}, \quad a_2 = \frac{\partial \eta}{\partial x}, \quad a_3 = \frac{\partial \xi}{\partial y}, \quad a_4 = \frac{\partial \eta}{\partial y},$$

$$\beta_1 = a_1^2 + a_3^2, \quad \beta_2 = a_2^2 + a_4^2, \quad \beta_3 = 2(a_1a_2 + a_3a_4),$$

$$\beta_4 = 2 \left(\frac{\partial^2 \xi}{\partial x^2} + \frac{\partial^2 \xi}{\partial y^2} \right), \quad \beta_5 = 2 \left(\frac{\partial^2 \eta}{\partial x^2} + \frac{\partial^2 \eta}{\partial y^2} \right) \quad (27)$$

As before, the velocity components u and v can be obtained using Eq (23). Also, the boundary conditions for solving Eqs (25) and (26) are as given in Eq (24).

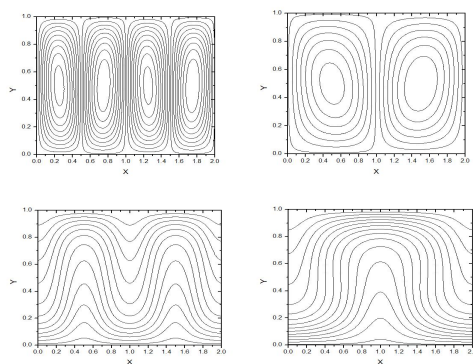


Fig 1. Streamlines (top) and Isotherms (bottom) for $Ar = 2, R_1 = R_2 = 100, \theta = 0^\circ$:
 Left: Isotropic, Right: Anisotropic

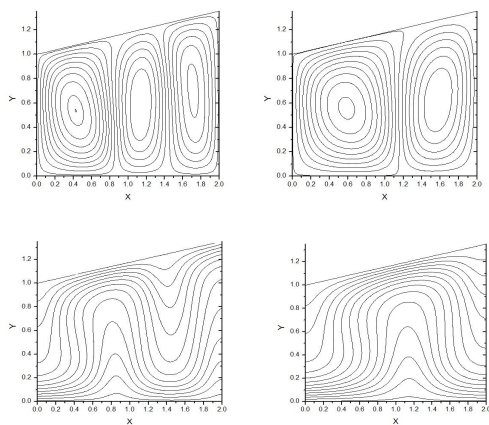


Fig 2. Streamlines (top) and Isotherms (bottom) for $Ar = 2, R_1 = R_2 = 100, \theta = 10^\circ$:
 Left: Isotropic, Right: Anisotropic

It may be noted that the solutions obtained in the unit square domain described by the above boundary value problems have to be transformed back to the physical trapezoidal domain. The details of the numerical solution procedure using a suitable finite difference method are available in our earlier works [18, 19], and are not given here, for brevity.

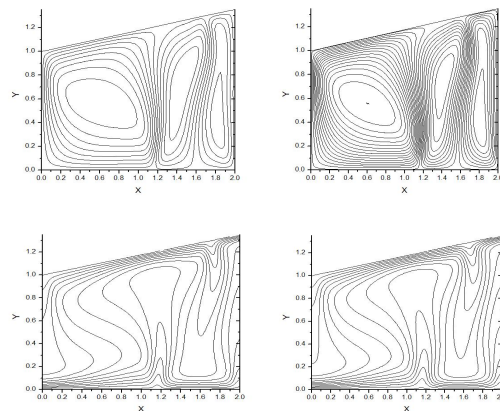


Fig 3. Streamlines (top) and Isotherms (bottom) for $Ar = 2, R_1 = R_2 = 500, \theta = 10^\circ$:
 Left: Isotropic, Right: Anisotropic

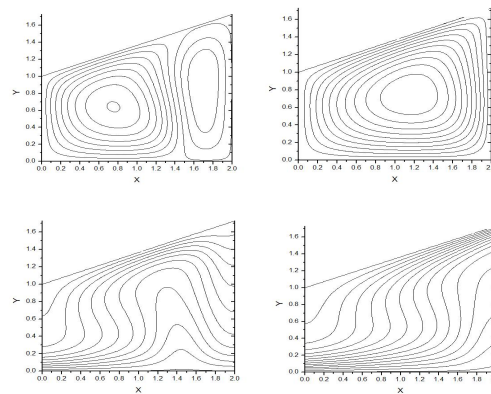


Fig 4. Streamlines (top) and Isotherms (bottom) for $Ar = 2, R_1 = R_2 = 100, \theta = 20^\circ$:
 Left: Isotropic, Right: Anisotropic

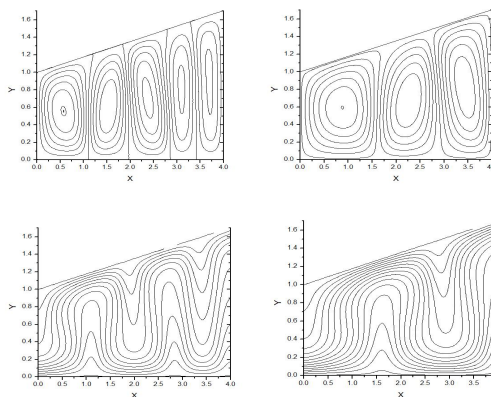


Fig 5. Streamlines (top) and Isotherms (bottom) for $Ar = 4, R_1 = R_2 = 100, \theta = 10^\circ$:
 Left: Isotropic, Right: Anisotropic

6. DISCUSSION

In natural convection studies involving finite enclosures, it is instructive to plot contours of streamlines and isotherms, and analyze their variations with the key flow parameters in order to assess the influence of geometrical and physical phenomena represented by these parameters. We have thus presented in this section some representative figures illustrating the variations of streamlines and isotherms for a host of parameters, namely, Rayleigh-Darcy number R_i , ($i = 1, 2$), inclination angle θ , and aspect ratio Ar . Since our emphasis in this study is to compare the hydrodynamical and thermal characteristics of the flow for isotropic vis-à-vis anisotropic porous media, we have assumed fixed values for the anisotropic parameters K ($= 1.2$) and α ($= 1.2$) in all illustrations.

Figures 1–5 exhibit the variations in streamlines and isotherms in the confines of the trapezoidal cavity for different values of Ar , R_i and θ . For ease of comparison, we have assumed that the Rayleigh-Darcy numbers R_1 (isotropic) and R_2 (anisotropic) are equal. In all figures, the top pair represent the streamlines while the bottom ones are the isotherms. Furthermore the left contours in each pair correspond to isotropic medium and the right ones relate to anisotropy.

In Fig 1, we have shown the plots for a rectangular cavity for fixed values of Ar ($= 2$), and $R_1 = R_2$ ($= 100$). It is apparent that isotropic and non-isotropic features significantly affect the ensuing fluid motion and convection currents. For instance, the streamline contours consist of four distinct loops for isotropic media while the anisotropic effect clearly changes the corresponding circulation pattern to two loops in the cavity. In other words, the fluid circulation pattern in an isotropic medium is profoundly checked by the anisotropy of the medium. A similar observation is prevalent for the isotherms as well. It is worth mentioning that the thermal convection currents dominate the whole cavity space for both types of porous media. However, the nature of the convection for an isotropic medium is a bit oscillatory as compared to the anisotropic counterpart.

The contours in Fig 2 correspond to a trapezoidal enclosure with the upper surface inclined at an angle of 10° to the horizontal, other parameters being the same as in Fig 1. Here also, the curves show qualitatively similar behavior as in Fig 1. However, the fluid circulation inside the non-rectangular cavity is altered, particularly for the isotropic medium. As regards the thermal convection, it is worth noting the formation of thin thermal boundary layers near the sloping surface.

In Fig 3, we have shown the streamlines and isotherms corresponding to $\theta = 10^\circ$, $Ar = 2$, and $R_1 = R_2$ ($= 500$). For higher values of Rayleigh-Darcy number, the circulations are broadly similar — nonetheless, intense — for both isotropic and anisotropic media. As regards isotherms, we observe that the patterns are strikingly similar. However, the convection currents are more confined to the upper and lower surfaces, in line with the thermal physics of the problem. It may also be noted in passing that the conduction effects are starting to be visible as the Rayleigh-Darcy number jumps to higher values.

In order to assess the effect of inclination angle of the upper

sloping surface on the circulation and convection currents, we have plotted in Fig 4 the level curves of stream function and temperature for $\theta = 20^\circ$. This figure has to be contrasted with Figs 1 and 2 in order to ascertain the effect of changing the upper surface slopes. In this comparison, it is quite apparent that the inclination of the upper surface indeed affects significantly both streamlines and isotherms. As regards the effect of isotropy versus anisotropy (cf. Fig 4), it is obvious that the nature of both fluid circulation as well as thermal currents of isotropic medium are grossly suppressed by anisotropic features. This again re-iterates our earlier observations.

The influence of changing the aspect ratio of the enclosure is depicted in the final figure 5. In this figure, we have shown the contours for $Ar = 4$ which corresponds to a doubling of the horizontal extent of the cavity vis-à-vis earlier illustrations. Once again, the fluid circulation (with 5 loops) for isotropic case dominates over the corresponding anisotropic circulation (3 loops). Similar behavior is apparent for isotherms. Moreover, the longer horizontal extent of the cavity results in more oscillations in the isotherms. In summary, we conclude that the anisotropy of the porous medium clearly suppresses the intensity of circulation as well as convection currents.

REFERENCES

- [1] Kvernfold, O., Tyvand, P.A., 1979, “Nonlinear thermal convection in anisotropic porous media”, *J. Fluid Mech.*, 90, pp. 609–624.
- [2] Ni, J., Beckermann, C., 1991, “Natural convection in a vertical enclosure filled with anisotropic porous media”, *J. Heat Transfer*, 113, pp. 1033–1037.
- [3] Chang, W.J., Liu, H.C., 1994, “Natural convection in a finite wall rectangular cavity filled with an anisotropic porous medium”, *Int. J. Heat Mass Transfer*, 37, pp. 303–312.
- [4] Kimura, S., Masuda, Y., Kazuo Hayashi, T., 1993, “Natural convection in an anisotropic porous medium heated from the side (effects of anisotropic properties of porous matrix)”, *Heat Transf. Jpn. Res.*, 22, pp. 139–153.
- [5] Friedman, S.P., Seaton, N.A., 1996, “On the transport properties of anisotropic networks of capillaries”, *Water Resources Res.*, 32, pp. 339–347.
- [6] Tyvand, P.A., Storesletten, L., 1991, “Onset of convection in an anisotropic porous medium with oblique principal axes”, *J. Fluid Mech.*, 226, pp. 371–382.
- [7] Storesletten, L., “Natural convection in a horizontal porous layer with anisotropic thermal diffusivity”, *Transp. Porous Media*, 12, pp. 19–29.
- [8] Degan, G., Vasseur, P., Bilgen, E., 1995, “Convective heat transfer in a vertical anisotropic porous layer”, *Int. J. Heat Mass Transfer*, 38, pp. 1975–1987.

- [9] Degan, G., Vasseur, P., 1996, "Natural convection in a vertical slot filled with an anisotropic porous medium with oblique principal axes", *Numer. Heat Transfer A*, 30, pp. 397–412.
- [10] Degan, G., Vasseur, P., 1997, "Boundary-layer regime in a vertical porous layer with anisotropic permeability and boundary effects", *Int. J. Heat Fluid Flow*, 18, pp. 334–343.
- [11] Zhang, X., 1993, "Convective heat transfer in a vertical porous layer with anisotropic permeability", *Proc. 14th Canadian Congress of Applied Mechanics*, 2, pp. 579–580.
- [12] Mamou, M., Mahidjida, A., Vasseur, P., Robillard, L., 1998, "Onset of convection in an anisotropic porous medium heated from below by a constant heat flux", *Int. Comm. Heat Mass Transfer*, 25, pp. 799–808.
- [13] Mahidjida, A., Robillard, L., Vasseur, P., Mamou, M., 2000, "Onset of convection in an anisotropic porous layer of finite lateral extent", *Int. Comm. Heat Mass Transfer*, 27, pp. 333–342.
- [14] Nithiarasu, P., Sujatha, K.S., Ravindran, K., Sundararajan, T., Seetharamu, K.N., 2000, "Non-Darcy natural convection in a hydrodynamically and thermally anisotropic porous medium", *Computer Meth. App. Mech. Engng.*, 188, pp. 413–430.
- [15] Wang, X., Thauvin, F., Mohanty, K.K., 1999, "Non-Darcy flow through anisotropic porous media", *Chem. Engng. Sci.*, 54, pp. 1859–1869.
- [16] Degan, G., Vasseur, P., Awanou, N.C., 2005, "Anisotropy effects on non-Darcy natural convection from concentrated heat sources in porous media", *Acta Mech.*, 179, pp. 111–124.
- [17] Jaya Krishna, D., Basak, T., Das, S.K., 2008, "Natural convection in a heat generating hydrodynamically and thermally anisotropic non-Darcy porous medium", *Int. J. Heat Mass Transfer*, 51, pp. 4691–4703.
- [18] Tiwari, A.K., Singh, A.K., Chandran, P., Sacheti, N.C., 2012, "Natural convection in a cavity with a sloping upper surface filled with an anisotropic porous material", *Acta Mech.*, 223, pp. 95–108.
- [19] Chandran, P., Sacheti, N.C., Singh, A.K., Bhadauria, B.S., 2016, "Steady free convection in an anisotropic porous non-rectangular vertical cavity", *Glob. J. Pure Appl. Math.*, 12, pp. 4799–4817.
- [20] Moretti, G., Abbett, M., 1966, "A time-dependent computational method for blunt body flows", *AIAA J.*, 4, pp. 2136–2141.
- [21] Smith, R.E., 1982, "Algebraic grid generation", In: Thompson, J. F. (ed.) *Numerical Grid Generation*. North Holland, Amsterdam.